CLEO CONF 96-2
ICHEP96 pa05-077

Measurement of Semileptonic B Meson Decay to P-Wave Charm Mesons

CLEO Collaboration

July 21, 1996

Abstract

We have studied semileptonic B meson decays with a P-wave charm meson in the final state using 2.8×10^6 $B\bar{B}$ events recorded by the CLEO II detector at the Cornell Electron-positron Storage Ring. We find a value for the exclusive semileptonic product branching fraction: $\mathcal{B}(B^- \to D_1^0 e^- \bar{\nu})\, \mathcal{B}(D_1^0 \to D^{*+}\pi^-) = (0.33 \pm 0.09 \pm 0.04)\%$ and an upper limit for $\mathcal{B}(B^- \to D_2^{*0} e^- \bar{\nu})\, \mathcal{B}(D_2^{*0} \to D^{*+}\pi^-) < 0.19\%$ (95% CL). These results indicate that at least 18% of the total B^- semileptonic rate is unaccounted for by the observed exclusive decays, $B^- \to D^0 \ell^- \bar{\nu}$, $B^- \to D^{*0} \ell^- \bar{\nu}$, $B^- \to D_1^0 \ell^- \bar{\nu}$ and $B^- \to D_2^{*0} \ell^- \bar{\nu}$.

T. E. Browder,[1] F. Li,[1] Y. Li,[1] J. L. Rodriguez,[1] T. Bergfeld,[2] B. I. Eisenstein,[2] J. Ernst,[2] G. E. Gladding,[2] G. D. Gollin,[2] E. Johnson,[2] I. Karliner,[2] M. Palmer,[2] M. Selen,[2] J. J. Thaler,[2] K. W. Edwards,[3] A. Bellerive,[4] D. I. Britton,[4] R. Janicek,[4] D. B. MacFarlane,[4] K. W. McLean,[4] P. M. Patel,[4] A. J. Sadoff,[5] R. Ammar,[6] P. Baringer,[6] A. Bean,[6] D. Besson,[6] D. Coppage,[6] C. Darling,[6] R. Davis,[6] N. Hancock,[6] S. Kotov,[6] I. Kravchenko,[6] N. Kwak,[6] S. Anderson,[7] Y. Kubota,[7] M. Lattery,[7] J. J. O'Neill,[7] S. Patton,[7] R. Poling,[7] T. Riehle,[7] A. Smith,[7] V. Savinov,[7] M. S. Alam,[8] S. B. Athar,[8] Z. Ling,[8] A. H. Mahmood,[8] H. Severini,[8] S. Timm,[8] F. Wappler,[8] A. Anastassov,[9] S. Blinov,[9,a] J. E. Duboscq,[9] R. Fulton,[9] D. Fujino,[9] K. K. Gan,[9] T. Hart,[9] K. Honscheid,[9] H. Kagan,[9] R. Kass,[9] J. Lee,[9] M. Sung,[9] A. Undrus,[9,a] R. Wanke,[9] A. Wolf,[9] M. M. Zoeller,[9] B. Nemati,[10] S. J. Richichi,[10] W. R. Ross,[10] P. Skubic,[10] M. Wood,[10] M. Bishai,[11] J. Fast,[11] E. Gerndt,[11] J. W. Hinson,[11] D. H. Miller,[11] E. I. Shibata,[11] I. P. J. Shipsey,[11] M. Yurko,[11] L. Gibbons,[12] S. D. Johnson,[12] Y. Kwon,[12] S. Roberts,[12] E. H. Thorndike,[12] C. P. Jessop,[13] K. Lingel,[13] H. Marsiske,[13] M. L. Perl,[13] S. F. Schaffner,[13] D. Ugolini,[13] R. Wang,[13] X. Zhou,[13] T. E. Coan,[14] V. Fadeyev,[14] I. Korolkov,[14] Y. Maravin,[14] I. Narsky,[14] V. Shelkov,[14] R. Stroynowski,[14] J. Staeck,[14] I. Volobouev,[14] J. Ye,[14] M. Artuso,[15] A. Efimov,[15] M. Gao,[15] M. Goldberg,[15] R. Greene,[15] F. Frasconi,[15] D. He,[15] S. Kopp,[15] G. C. Moneti,[15] R. Mountain,[15] Y. Mukhin,[15] S. Schuh,[15] T. Skwarnicki,[15] S. Stone,[15] X. Xing,[15] J. Bartelt,[16] S. E. Csorna,[16] V. Jain,[16] S. Marka,[16] A. Freyberger,[17] R. Godang,[17] D. Gibaut,[17] K. Kinoshita,[17] I. C. Lai,[17] P. Pomianowski,[17] S. Schrenk,[17] G. Bonvicini,[18] D. Cinabro,[18] L. Perera,[18] B. Barish,[19] M. Chadha,[19] S. Chan,[19] G. Eigen,[19] J. S. Miller,[19] C. O'Grady,[19] M. Schmidtler,[19] J. Urheim,[19] A. J. Weinstein,[19] F. Würthwein,[19] D. M. Asner,[20] D. W. Bliss,[20] W. S. Brower,[20] G. Masek,[20] H. P. Paar,[20] J. Gronberg,[21] C. M. Korte,[21] D. J. Lange,[21] R. Kutschke,[21] S. Menary,[21] R. J. Morrison,[21] S. Nakanishi,[21] H. N. Nelson,[21] T. K. Nelson,[21] C. Qiao,[21] J. D. Richman,[21] D. Roberts,[21] A. Ryd,[21] H. Tajima,[21] M. S. Witherell,[21] R. Balest,[22] B. H. Behrens,[22] K. Cho,[22] W. T. Ford,[22] H. Park,[22] P. Rankin,[22] J. Roy,[22] J. G. Smith,[22] J. P. Alexander,[23] C. Bebek,[23] B. E. Berger,[23] K. Berkelman,[23] K. Bloom,[23] D. G. Cassel,[23] H. A. Cho,[23] D. M. Coffman,[23] D. S. Crowcroft,[23] M. Dickson,[23] P. S. Drell,[23] R. Ehrlich,[23] R. Elia,[23] A. D. Foland,[23] P. Gaidarev,[23] B. Gittelman,[23] S. W. Gray,[23] D. L. Hartill,[23] B. K. Heltsley,[23] P. I. Hopman,[23] S. L. Jones,[23] J. Kandaswamy,[23] N. Katayama,[23] P. C. Kim,[23] D. L. Kreinick,[23] T. Lee,[23] Y. Liu,[23] G. S. Ludwig,[23] J. Masui,[23] J. Mevissen,[23] N. B. Mistry,[23] C. R. Ng,[23] E. Nordberg,[23] M. Ogg,[23,b] J. R. Patterson,[23] D. Peterson,[23] D. Riley,[23] A. Soffer,[23] C. Ward,[23] P. Avery,[24] M. Athanas,[24] C. D. Jones,[24] M. Lohner,[24] C. Prescott,[24] S. Yang,[24] J. Yelton,[24] J. Zheng,[24] G. Brandenburg,[25] R. A. Briere,[25] D. Y.-J. Kim,[25] T. Liu,[25] M. Saulnier,[25] R. Wilson,[25] and H. Yamamoto[25]

[1]*University of Hawaii at Manoa, Honolulu, Hawaii 96822*
[2]*University of Illinois, Champaign-Urbana, Illinois 61801*
[3]*Carleton University, Ottawa, Ontario, Canada K1S 5B6*
and the Institute of Particle Physics, Canada
[4]*McGill University, Montréal, Québec, Canada H3A 2T8*
and the Institute of Particle Physics, Canada

[a]Permanent address: BINP, RU-630090 Novosibirsk, Russia.
[b]Permanent address: University of Texas at Austin.

[5]Ithaca College, Ithaca, New York 14850
[6]University of Kansas, Lawrence, Kansas 66045
[7]University of Minnesota, Minneapolis, Minnesota 55455
[8]State University of New York at Albany, Albany, New York 12222
[9]Ohio State University, Columbus, Ohio 43210
[10]University of Oklahoma, Norman, Oklahoma 73019
[11]Purdue University, West Lafayette, Indiana 47907
[12]University of Rochester, Rochester, New York 14627
[13]Stanford Linear Accelerator Center, Stanford University, Stanford, California 94309
[14]Southern Methodist University, Dallas, Texas 75275
[15]Syracuse University, Syracuse, New York 13244
[16]Vanderbilt University, Nashville, Tennessee 37235
[17]Virginia Polytechnic Institute and State University, Blacksburg, Virginia 24061
[18]Wayne State University, Detroit, Michigan 48202
[19]California Institute of Technology, Pasadena, California 91125
[20]University of California, San Diego, La Jolla, California 92093
[21]University of California, Santa Barbara, California 93106
[22]University of Colorado, Boulder, Colorado 80309-0390
[23]Cornell University, Ithaca, New York 14853
[24]University of Florida, Gainesville, Florida 32611
[25]Harvard University, Cambridge, Massachusetts 02138

1 Introduction

There is general agreement among a number of measurements [1] of the exclusive semileptonic $\bar{B}$ meson decays, $\bar{B} \to D\ell^-\bar{\nu}$ and $\bar{B} \to D^*\ell^-\bar{\nu}$. Together they account for approximately 60 – 70% of the inclusive $\bar{B} \to X\ell^-\bar{\nu}$ branching fraction [1]. This is illustrated by the measurements [2, 3, 4] given in Table 1. Since the branching fraction for $b \to u\ell\bar{\nu}$ is known to be small, the missing exclusive decays must be sought among $b \to c\ell\bar{\nu}$ decays to higher mass D_J states or nonresonant [5] hadronic states with a D or D^* and other hadrons. Measurements of $B^- \to D_1^0\ell^-\bar{\nu}$ and $B^- \to D_2^{*0}\ell^-\bar{\nu}$ have been reported previously [6, 7]. In this paper we report new measurements of these two decay modes. A more complete description of these results can be found in Ref. [8].

The D_J mesons contain one charm quark and one light quark with relative angular momentum $L = 1$. The quark spins can sum to $S = 0$ or $S = 1$, and consequently there are four spin-parity states given by $J^P = 1^+$ or $0^+, 1^+, 2^+$. Parity and angular momentum conservation restrict the decays available to the four states. The 2^+ state may decay to either $D\pi$ or $D^*\pi$ through D-wave decays and both 1^+ states may decay only to $D^*\pi$ through S or D-wave decay, while the 0^+ state can decay only to $D\pi$ and must go through S-wave decay.

According to Heavy Quark Effective Theory (HQET), there exists an approximate spin-flavor symmetry for hadrons consisting of one heavy and one light quark [9]. In the limit of infinite heavy quark mass, such mesons are described by the quantum numbers $j = S_q + L$ (the total angular momentum of the light constituents), S_Q (the spin of the heavy quark), and $J = j + S_Q$ (the spin of the meson). In HQET, the D_J mesons make up two doublets, $j = 1/2$ and $j = 3/2$. The members of the $j = 3/2$ doublet are predicted to decay only in a D-wave and to be relatively narrow. The $j = 1/2$ mesons are predicted to decay only in an S-wave and to be relatively broad. In this analysis we study the semileptonic decays of the B meson to final states containing the narrow (j=3/2) excited charm mesons: the ${}^{j}L_J = {}^{3/2}P_2$ and ${}^{3/2}P_1$, labeled by the Particle Data Group and referred to here as the D_2^* and D_1, respectively.

2 Event Selection

The data used in this analysis were produced in e^+e^- collisions at the Cornell Electron-positron Storage Ring (CESR) and recorded with the CLEO II detector. The data sample consists of 2.79×10^6 $B\bar{B}$ events collected at the $\Upsilon(4S)$ center-of-mass energy. A detailed description of the CLEO II detector is given elsewhere [10]. For this analysis we select hadronic events [11] that have at least one track identified as an electron with momentum between 0.8 GeV/c and 2.0 GeV/c. Electron candidates are required to lie within the region $|\cos\theta_e| < 0.91$, where θ_e is the angle of the electron candidate with respect to the beam axis. Electrons are identified by matching energy deposition in the CsI calorimeter and momentum measured in the drift chamber, their energy loss in the drift chamber gas (dE/dx) and their time of flight in the detector. The lower limit on their momentum for this analysis is determined by our lepton identification capabilities and the upper limit is the kinematic limit for the electron in $B^- \to (D_1^0 \text{ or } D_2^{*0})\ell^-\bar{\nu}$. We do not use muons for this analysis because the hadron misidentification rate for muons with momenta below 1.4 GeV/c is high and most of the leptons from semileptonic B decays to excited charm mesons are below that momentum.

For each electron in these events we search for D_J^0 candidates in the decay chain $D_J^0 \to D^{*+}\pi^-$, $D^{*+} \to D^0\pi^+, D^0 \to K^-\pi^+$ or $D^0 \to K^-\pi^+\pi^0$ [12]. All charged tracks in the decay chain must originate from the vicinity of the e^+e^- interaction point and, with the exception of the slow pion from the decay of the D^{*+}, have measured ionization losses in the drift chamber within 2.5σ (standard deviations) of those expected for the hypothesis under consideration. We also take advantage of the charge correlation with the electron from the B semileptonic decay and the K^- in the D^0 decay, and require the kaon candidate and the electron candidate to have the same sign.

In the search for D^0 decays in the modes $D^0 \to K^-\pi^+$ and $D^0 \to K^-\pi^+\pi^0$, we require that each D^0 candidate have a momentum consistent with being a B meson decay product; that is, the D^0 candidate must have $x_D < 0.5$, where $x_D = p_D/(E_{\text{beam}}^2 - M_D^2)^{\frac{1}{2}}$ is the D^0 momentum (p_D) divided by the momentum of a D^0 with the beam energy. In the $D^0 \to K^-\pi^+$ mode, $K^-\pi^+$ candidates must have an invariant mass within 1.5σ (11 MeV/c^2) of the known D^0 mass. For the $D^0 \to K^-\pi^+\pi^0$ mode, the π^0 is identified using the CsI calorimeter using the following conditions: each of the two photons is required to have an energy of at least 50 MeV and the $\gamma\gamma$ invariant mass $M_{\gamma\gamma}$ must be within 10 MeV/c^2 of the known π^0 mass. The momenta and energies of the $\gamma\gamma$ pairs that satisfy these requirements are then subjected to a kinematic fit with $M_{\gamma\gamma}$ constrained to the π^0 mass. We enforce that each π^0 must have a minimum energy of $E_{\pi^0}^{\min} = (p_{\pi^0}^2 + M_{\pi^0}^2)^{\frac{1}{2}} = 350$ MeV. We also require that each $D^0 \to K^-\pi^+\pi^0$ candidate must have the invariant mass of the $K^-\pi^+\pi^0$ combination within 1.5σ (22.5 MeV/c^2) of the known D^0 mass.

To reduce the combinatorial background in reconstructing the $D^0 \to K^-\pi^+\pi^0$ decay, we use results from E691 [13] to compute a Dalitz plot probability weight for each $K^-\pi^+\pi^0$ combination. We settle on a minimum acceptable value for this weight chosen to maximize signal over background using signal Monte Carlo events and background from data. The Dalitz plot weight requirement accepts 70% of the real $D^0 \to K^-\pi^+\pi^0$ decays and rejects 75% of the fake D^0's. Finally, for this mode, we require $p_D > 0.8$ GeV/c in order to further reject fake D^0 background.

We then combine D^0 candidates with π^+ candidates to form D^{*+} candidates. The slow pion used to form the D^{*+} must have a momentum of at least 65 MeV/c and the D^{*+} candidate must have $x_{D^*} < 0.5$, where x_{D^*} for the D^{*+} candidate is defined in the same manner as x_D for the D^0 candidate. For each D^{*+} candidate we calculate a mass difference, $\delta M \equiv M(D^0\pi^+) - M(D^0)$. The D^{*+} candidates with a value of δM within 2σ (2 MeV/c^2) of the known $D^{*+} - D^0$ mass difference are then combined with an additional charged pion in the event to form a D_J^0 candidate.

These D_J^0 candidates are then paired with electrons selected as described above to form candidates for $B^- \to D_J^0 e^- \bar{\nu}$ decays. The energy ($E_{D_J e}$) and momentum ($\mathbf{p}_{D_J e}$) of each $D_J^0 e^-$ candidate are then computed from the energies and momenta of the D_J^0 and e^- candidates.

There is significant background in this analysis from real D^{*+}'s combined with pions that are not from D_J^0 mesons. To suppress this background we select D_J^0 e^- pairs that are consistent with $B^- \to D_J^0 e^- \bar{\nu}$ decays and reject D_J^0 e^- pairs that are consistent with $\bar{B}^0 \to D^{*+} e^- \bar{\nu}$. Using the beam energy constraint $E_{\text{beam}} = E_B = E_{D_J e} + E_\nu$ and the B meson mass [14], we can compute the energy and the momentum of the neutrino in $B^- \to D_J^0 e^- \bar{\nu}$. Although we do not know the direction of the B meson or the $\bar{\nu}$, we can use $\mathbf{p}_B = \mathbf{p}_{D_J e} + \mathbf{p}_\nu$, to construct the angle $\theta_{D_J e}$ between the momenta of the B and the $D_J^0 e^-$:

$$\cos\theta_{D_J e} = \frac{p_{D_J e}^2 + p_B^2 - p_\nu^2}{2 p_B p_{D_J e}}. \tag{1}$$

For true $B^- \to D_J^0 e^- \bar{\nu}$ decays, measured in a perfect detector, $\cos\theta_{D_J e}$ will have physical values, $|\cos\theta_{D_J e}| \leq 1$. Due to measurement errors, some candidates will have slightly non-physical values of $\cos\theta_{D_J e}$. For decays in which either particles from the B decay chain are missing (*e.g.*, $B \to D_J^0 X e^- \bar{\nu}$) or for combinatoric background events when an extra random pion has been added to a true semileptonic B decay with a D^{*+} in the final state, $\cos\theta_{D_J e}$ is shifted toward nonphysical values. Figure 1 illustrates Monte Carlo distributions of $\cos\theta_{D_J e}$ for $B^- \to D_J^0 e^- \bar{\nu}$ and for generic $B\bar{B}$ background events. We require D_J^0 e^- candidates to have $|\cos\theta_{D_J e}| \leq 1$. This requirement retains 93% of the $B^- \to D_J^0 e^- \bar{\nu}$ decays and eliminates 62% of the background from real D^{*+}'s combined with pions that are not from D_J^0 mesons.

Similarly, we construct the angle $\theta_{D^* e}$, between the B and the D^{*+} e^- momentum:

$$\cos\theta_{D^* e} = \frac{p_{D^* e}^2 + p_B^2 - p_\nu^2}{2 p_B p_{D^* e}}. \tag{2}$$

For true $\bar{B}^0 \to D^{*+} e^- \bar{\nu}$ decays, measured in a perfect detector, $|\cos\theta_{D^* e}| \leq 1$. Due to measurement errors some signal candidates will have slightly non-physical values of $\cos\theta_{D^* e}$. For $B^- \to D_J^0 e^- \bar{\nu}$ decays, in which the correct D^{*+} and electron have been used (and the

D_J^0 daughter π^- has been ignored) in the computation of p_ν, $\cos\theta_{D^*e}$ is shifted toward negative values as illustrated in Figure 2. We therefore require $\cos\theta_{D^*e} < -1$. This cut substantially reduces the dominant background to this analysis which comes from true $\bar{B}^0 \to D^{*+}e^-\bar{\nu}$ decays, where the D^{*+} is combined with a random pion in the event to make a D_J^0 candidate. This requirement retains 70% of the $B^- \to D_J^0 e^-\bar{\nu}$ decays and eliminates 91% of the background from true $\bar{B}^0 \to D^{*+}e^-\bar{\nu}$ decays.

The angles $\theta_{D_J e}$ and θ_{D^*e} are correlated – when the requirements $|\cos\theta_{D_J e}| \leq 1$ and $\cos\theta_{D^*e} < -1$ are applied together, they retain 65% of the $B^- \to D_J^0 e^-\bar{\nu}$ decays and reject 88% of the background remaining after all other cuts.

3 Yields and Backgrounds

After applying all the requirements described above, a histogram of the mass difference $\delta m_J \equiv M(D^{*+}\pi^-) - M(D^{*+})$ is made containing one entry for each candidate $D_J^0\ e^-$ pair, potentially with multiple entries per event. The combined data for both decay modes of the D^0 meson and the fit described below are shown in Figure 3.

This histogram is fit to a background function plus Breit-Wigner resonance functions corresponding to the lineshapes of the two narrow D_J^0 resonances [15]. Each Breit-Wigner function is convoluted with a Gaussian that describes the detector resolution. The resonance parameters used in the fit are given in Table 2. The width of the Gaussian is estimated by Monte Carlo calculation to be 4 MeV/c^2. The background is described by a polynomial in δm_J consisting of half-integer powers with a root at the kinematic limit, the pion mass. The fit is actually performed using narrow histogram bins of width 1 MeV/c^2 in order to ensure that the choice of bin width does not affect the results. The solid line in Figure 3 illustrates the results of the fit. The fit gives a good confidence level. To check that the data are consistent with the presence of a signal, we fitted the δm_J distribution with only the smooth background function. The increase in the logarithmic likelihood of the fit with only the background functions over that of the fit with both the signal and background functions is 21 (for an increase of 2 d.o.f.), which indicates a significant signal over the background. While, there is a statistically significant enhancement in the region of the narrow D_1^0 resonance at $\delta m_J = 0.411$ GeV/c^2, the evidence for a signal for the other narrow resonance, D_2^{*0}, at $\delta m_J = 0.455$ GeV/c^2 is not compelling.

Yields and branching fractions are also obtained by fitting the $D^0 \to K^-\pi^+$ and $D^0 \to K^-\pi^+\pi^0$ data separately. The branching fractions obtained by averaging the results from separate fits agree with the results of the simultaneous fit to both modes within two significant figures. Since the systematic errors of the two D^0 modes are somewhat different, we present the analysis of the fits to the two separate modes. The yields obtained from the separate fits are given in Table 3.

The contamination of our data from non-$B\bar{B}$ events is obtained by measuring the signal yield using "OFF resonance" data, *i.e.*, data taken at energies slightly below the $\Upsilon(4S)$ resonance. The results are scaled by the ratio of the luminosities and the square of the beam energies (ON and OFF resonance) and subtracted from our yield obtained by fitting the ON resonance data. The final yields are given in Table 3.

To study the remaining backgrounds we use 6.7×10^6 generic $B\bar{B}$ Monte Carlo events in which the B mesons are allowed to decay through all available channels, constrained by the Standard Model and the measured branching fractions. Such a sample enables us to see how much background other processes contribute to our measurement and how our cuts affect their contributions. The background in Figure 3 is predicted by generic $B\bar{B}$ Monte Carlo to be dominated by combinatoric background in which a real electron and a real D^{*+} combine with a random pion in the event pass all selection criteria. According to Monte Carlo, such combinatoric background accounts for 82% of the background to our signal in the $D^0 \to K^-\pi^+$ mode, the remainder being misreconstructed D^{*+}'s. For the $D^0 \to K^-\pi^+\pi^0$ mode the real D^{*+} background accounts for 57% of the background. The combinatoric background is also well modeled, both in Monte Carlo and in data, by a sample of events that pass the same selection criteria as our signal except that, in forming the D_J^0 candidate, a D^{*+} and a wrong sign pion (a pion with the same sign as the D^{*+}) are used. This wrong sign Monte Carlo sample is shown as the dashed histograms in Figures 4(a) and (c). Figures 4(b) and (d) show the difference between the right sign MC signal sample and the wrong sign background MC sample. In addition, both the shape and magnitude of the right sign and wrong sign Monte Carlo backgrounds agree well with the corresponding backgrounds in the data.

Backgrounds due to misidentification of a hadron as an electron or in which a D_J^0 is paired with an electron from the other B are negligible [8]. We make no attempt to subtract backgrounds due to other misreconstruction problems. Furthermore, we are not able to subtract contributions from other processes, such as semileptonic decays to broad or non-resonant $D^{*+}X$ states or other $B \to D_J^0 X e^- \bar{\nu}$ decays, since we have no experimental handle to distinguish these possible contributions from background.

4 Efficiencies

Our event selection efficiencies were obtained using Monte Carlo events generated with either $B^- \to D_1^0 e^- \bar{\nu}$ or $B^- \to D_2^{*0} e^- \bar{\nu}$ and containing one signal decay per event. The Monte Carlo events were generated according to the ISGW model [16] and were passed through a GEANT based simulation of the detector. The entire procedure applied to the data was carried out on this Monte Carlo sample and the final signal yield divided by the number of events generated was interpreted as the efficiency. The δm_J distributions for signal Monte Carlo events are shown in Figure 5, where the fits shown are made following the same procedure as the fits to the ON resonance data. The efficiencies are given in Table 4. The quoted errors on the efficiencies are statistical only.

5 Calculation of the Branching Fractions

The product branching fractions, $\mathcal{B}(B^- \to D_1^0 e^- \bar{\nu})\,\mathcal{B}(D_1^0 \to D^{*+}\pi^-)$ and an upper limit on $\mathcal{B}(B^- \to D_2^{*0} e^- \bar{\nu})\,\mathcal{B}(D_2^{*0} \to D^{*+}\pi^-)$ are calculated by correcting the observed yields with the signal reconstruction efficiency and dividing by the total number $N_{\Upsilon(4S)}$ of $\Upsilon(4S)$ decays in our data sample. We assume that the branching fractions of $\Upsilon(4S)$ to charged and neutral $B\bar{B}$ pairs are each 50%. From our yields the product branching fractions are then computed using:

$$\mathcal{B}(B^- \to D_J^0 e^- \bar{\nu})\, \mathcal{B}(D_J^0 \to D^{*+}\pi^-) = \frac{n(D_J)/\varepsilon_J}{N_{\Upsilon(4S)}\, \mathcal{B}(D^{*+} \to D^0\pi^+)\, \mathcal{B}(D^0 \to K^-\pi^+(\pi^0))}. \tag{3}$$

The values of the D^{*+} [17] and D^0 [14, 18] branching fractions that we use are:

$$\begin{aligned} \mathcal{B}(D^{*+} \to D^0\pi^+) &= (68.1 \pm 1.6)\% && (4)\\ \mathcal{B}(D^0 \to K^-\pi^+) &= (3.91 \pm 0.19)\% && (5)\\ \mathcal{B}(D^0 \to K^-\pi^+\pi^0) &= (13.8 \pm 1.0)\%. && (6) \end{aligned}$$

We choose to quote the product of branching fractions because the branching fractions for $D_J^0 \to D^{*+}\pi^-$ have not been measured. We determine a value for the product branching fractions from each of the D^0 decay modes and average the two measurements for a final value. The contributions of the important systematic errors are listed in Table 5. The systematic error associated with the model dependence of the efficiency is not included. With these systematic errors, the product branching fractions are:

$$\begin{aligned} \mathcal{B}(B^- \to D_1^0 e^- \bar{\nu})\, \mathcal{B}(D_1^0 \to D^{*+}\pi^-) &= (0.33 \pm 0.09 \pm 0.04)\ \% && (7)\\ \mathcal{B}(B^- \to D_2^{*0} e^- \bar{\nu})\, \mathcal{B}(D_2^{*0} \to D^{*+}\pi^-) &< 0.19\ \%\ \ (95\%\ \mathrm{CL}). && (8) \end{aligned}$$

The first error on $\mathcal{B}(B^- \to D_1^0 e^- \bar{\nu})\, \mathcal{B}(D_1^0 \to D^{*+}\pi^-)$ is statistical and the second is systematic. These results are also given in Table 3.

In order to estimate the contribution of these decays to the total semileptonic B meson branching fraction, we need to make some assumptions about the branching fractions of the D_J^0 mesons. Isospin conservation and recent CLEO measurements [15] of the decays of the D_J^0 mesons suggest that $\mathcal{B}(D_1^0 \to D^{*+}\pi^-) = 67\%$ and $\mathcal{B}(D_2^{*0} \to D^{*+}\pi^-) = 20\%$. Using these estimates we find:

$$\begin{aligned} \mathcal{B}(B^- \to D_1^0 e^- \bar{\nu}) &= (0.49 \pm 0.13 \pm 0.06)\ \% && (9)\\ \mathcal{B}(B^- \to D_2^{*0} e^- \bar{\nu}) &< 1.0\ \%\ \ (95\%\ \mathrm{CL}). && (10) \end{aligned}$$

In Table 6, these results are compared with recent results from other experiments. A clear picture of the exclusive modes which make up the 30 – 40% of the B semileptonic decays that are not $D\ell\nu$ and $D^*\ell\nu$ has not yet emerged. However, it appears that no more than half of the excess can be due to exclusive semileptonic decays to $D_1^0(2420)$ and $D_2^{*0}(2460)$.

6 Conclusions

In summary, we have studied exclusive semileptonic decays of the B mesons to P-wave charm mesons. We measured a branching fraction for $\mathcal{B}(B^- \to D_1^0 e^- \bar{\nu})\, \mathcal{B}(D_1^0 \to D^{*+}\pi^-)$ and an upper limit for $\mathcal{B}(B^- \to D_2^{*0} e^- \bar{\nu})\mathcal{B}(D_2^{*0} \to D^{*+}\pi^-)$. These results indicate that a substantial fraction ($\gtrsim$18%) of the inclusive B semileptonic rate is from modes other than $D\ell\nu$, $D^*\ell\nu$, $D_1\ell\nu$ and $D_2^*\ell\nu$.

7 Acknowledgments

We gratefully acknowledge the effort of the CESR staff in providing us with excellent luminosity and running conditions. J.P.A., J.R.P., and I.P.J.S. thank the NYI program of the NSF, M.S thanks the PFF program of the NSF, G.E. thanks the Heisenberg Foundation, K.K.G., M.S., H.N.N., T.S., and H.Y. thank the OJI program of DOE, J.R.P, K.H., and M.S. thank the A.P. Sloan Foundation, and A.W., and R.W. thank the Alexander von Humboldt Stiftung for support. This work was supported by the National Science Foundation, the U.S. Department of Energy, the Natural Sciences and Engineering Research Council of Canada and le Fonds Québécois pour la Formation de Chercheurs et l'Aide à la Recherche.

References

[1] Jeffrey D. Richman and Patricia R. Burchat, Rev. Mod. Phys. **67**, 893 (1995).

[2] CLEO Collaboration, CLEO-CONF-95-10, EPS0166 (1995).

[3] CLEO Collaboration, B. Barish *et al.*, Phys. Rev. **D51**, 1014 (1995).

[4] CLEO Collaboration, B. Barish *et al.*, Phys. Rev. Lett. **76**, 1570 (1996).

[5] Hai-Yang Cheng *et al.*, Phys. Rev. **D48**, 3204 (1993).

[6] ALEPH Collaboration, D. Buskulic *et al.*, Phys. Lett. **B345**, 103 (1995).

[7] OPAL Collaboration, R. Akers *et al.*, Z. Phys. **C69**, 57 (1995).

[8] S.L. Jones, Ph.D. thesis, Cornell University, 1996.

[9] N. Isgur and M.B. Wise, Phys. Rev. Lett. **66**, 1130 (1991); M. Lu, M. Wise and N. Isgur, Phys. Rev. **D45**, 1553 (1992); M. Neubert, Phys Reports **245**, 259 (1994).

[10] Y. Kubota *et al.*, Nucl. Instrum. Methods Phys. Res., Sect. A **320**, 66 (1992).

[11] To be classified as hadronic, an event must have at least 3 charged tracks originating near the interaction point, and the total visible energy for the event must be greater than $0.15E_{CM}$, where E_{CM} is the center-of-mass energy.

[12] Here and throughout the paper, charged conjugate modes are implied.

[13] E691 Collaboration, J.C Anjos *et al.*, Phys. Rev. **D48**, 56 (1994).

[14] Particle Data Group, L. Montanet *et al.*, Phys. Rev. **D50**, 1173 (1994).

[15] CLEO Collaboration, P. Avery *et al.*, Phys. Lett. **B331**, 236 (1994).

[16] N. Isgur, D. Scora, B. Grinstein and M. Wise, Phys. Rev. **D39**, 799 (1989).

[17] CLEO Collaboration, F. Butler *et al.*, Phys. Rev. Lett **69**, 2041 (1992).

[18] CLEO Collaboration, D. S. Akerib *et al.*, Phys. Rev. Lett **71**, 3070 (1993). CLEO reports two values for $\mathcal{B}(D^0 \to K^+\pi^-)$, a value obtained using efficiencies from a Monte Carlo simulation that does not include final state radiation and a value obtained using efficiencies from a Monte Carlo simulation that does include final state radiation. We use the former, because our Monte Carlo simulation of D^0 decays did not include final state radiation.

Table 1: The CLEO measurements [2, 3] of the exclusive semileptonic branching ratios $B^- \to D^0 e^- \bar{\nu}$ and $B^- \to D^{*0} e^- \bar{\nu}$ and measurement [4] of the inclusive semileptonic branching fraction of the B meson. Note that all results use the same value for the $D^0 \to K^-\pi^+$ branching fraction [18]. Over 30% of the inclusive semileptonic branching fraction is not accounted for by decays to the lowest pseudoscalar and vector charm mesons.

Decay Mode	Branching Fraction	Reference
$B^- \to D^0 e^- \bar{\nu}$	$(1.95 \pm 0.55)\%$	[2]
$B^- \to D^{*0} e^- \bar{\nu}$	$(5.13 \pm 0.84)\%$	[3]
$\mathcal{B}(B \to X e^- \bar{\nu})$	$(10.49 \pm 0.46)\%$	[4]
Inclusive - Exclusive	$(3.4 \pm 1.1)\%$	

Table 2: The parameters of the Breit-Wigner resonance functions that are used in the fits to describe the D_1^0 and D_2^{*0} resonances. In the fit the resonance function is convoluted with a Gaussian of width 4 MeV/c^2 to describe the detector resolution.

Resonance	δm_J (GeV/c^2)	Γ (GeV/c^2)	Reference
D_1^0	$0.411^{+0.002}_{-0.003}$	$0.020^{+0.007}_{-0.006}$	[15]
D_2^{*0}	0.455 ± 0.004	$0.028^{+0.010}_{-0.009}$	[15]

Table 3: Yields and product branching fractions. The "Final Yields" are given after the subtraction of the results of the OFF Resonance fits from the ON Resonance fits. The first error is statistical and the second is systematic.

$\mathcal{B}(B^- \to D_1^0 e^- \bar{\nu})\, \mathcal{B}(D_1^0 \to D^{*+}\pi^-)$		
	$K^-\pi^+$	$K^-\pi^+\pi^0$
ON Resonance Yield	25 ± 8	14 ± 7
OFF Resonance Yield	2 ± 2	0 ± 1
Final Yield	23 ± 8	14 ± 7
Product $\mathcal{B}$	$(0.33 \pm 0.11 \pm 0.05)$ %	$(0.33 \pm 0.17 \pm 0.07)$ %
Average Product $\mathcal{B}$	$(0.33 \pm 0.09 \pm 0.04)$ %	

$\mathcal{B}(B^- \to D_2^{*0} e^- \bar{\nu})\, \mathcal{B}(D_2^{*0} \to D^{*+}\pi^-)$		
	$K^-\pi^+$	$K^-\pi^+\pi^0$
ON Resonance Yield	0 ± 7	3 ± 6
OFF Resonance Yield	0 ± 2	0 ± 2
Final Yield	0 ± 7	3 ± 6
Product $\mathcal{B}$	$(0.00 \pm 0.10 \pm 0.02)$ %	$(0.08 \pm 0.16 \pm 0.03)$ %
Average Product $\mathcal{B}$	$(0.02 \pm 0.09 \pm 0.02)$ %	
Upper Limit	< 0.19 % (95% CL)	

Table 4: Reconstruction efficiencies ε_J for $B^- \to D_J^0 e^- \bar{\nu}$ decays for each of the D^0 decay modes used in the reconstruction.

	D^0 Decay Mode	
Efficiency	$D^0 \to K^-\pi^+$	$D^0 \to K^-\pi^+\pi^0$
$\varepsilon_1 \equiv \varepsilon(B^- \to D_1^0 e^- \bar{\nu})$	(9.46 ± 0.27) %	(1.61 ± 0.09) %
$\varepsilon_2 \equiv \varepsilon(B^- \to D_2^{*0} e^- \bar{\nu})$	(9.08 ± 0.26) %	(1.36 ± 0.09) %

Table 5: Systematic errors on the branching fraction (or upper limit) results, given in %. Particle Efficiency includes the charged particle tracking and electromagnetic calorimeter efficiencies for all particles other than the slow π. The systematic error on the Dalitz probability weight cut ($K\pi\pi^0$ mode only) is included in the systematic errors on ε_1 and ε_2.

Source	D_1^0 Yield		D_2^{0*} Yield	
	$K^-\pi^+$	$K^-\pi^+\pi^0$	$K^-\pi^+$	$K^-\pi^+\pi^0$
M_{D_J} & Γ_{D_J}	4%	7%	8%	1%
Background Function	8%	14%	8%	7%
$\cos\theta_{D_J e}$ and $\cos\theta_{D^* e}$	6%	6%	6%	6%
ε_1 and ε_2	3%	7%	3%	8%
$\mathcal{B}(D^{*+} \to D^0\pi^+)$	2%	2%	2%	2%
$\mathcal{B}(D^0)$	5%	7%	5%	7%
Slow π Efficiency	5%	5%	5%	5%
Particle Efficiency	4%	5%	4%	5%
Luminosity	2%	2%	2%	2%
Total	14%	21%	16%	16%

Table 6: Comparison of experimental values for the branching fractions. The first error listed is statistical and the second systematic. All results are given in %.

	$\mathcal{B}(B^- \to D_1^0 e^- \bar{\nu})$	$\mathcal{B}(B^- \to D_2^{*0} l^- \bar{\nu})$	Reference
ALEPH	$(0.76 \pm 0.22 \pm 0.13)$ %	< 1.0 % (95% CL)	[6]
OPAL	$(2.02 \pm 0.51 \pm 0.47)$ %	$(0.88 \pm 0.35 \pm 0.18)$ %	[7]
CLEO	$(0.49 \pm 0.13 \pm 0.06)$ %	< 1.0 % (95% CL)	This Paper

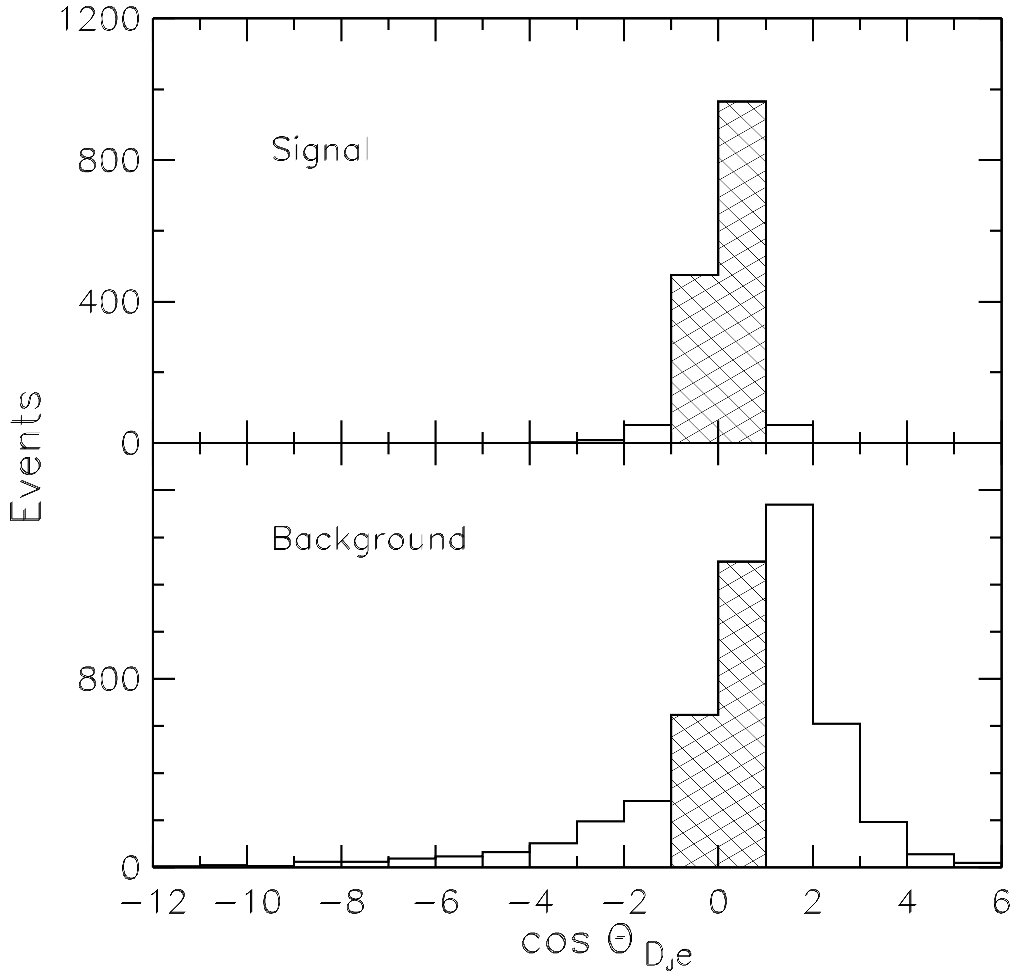

Figure 1: The value of $\cos\theta_{D_J e}$ is plotted for tagged Monte Carlo signal events and generic Monte Carlo background from the $D^0 \to K^-\pi^+$ mode. (The angle $\theta_{D_J e}$ is the angle between the momentum of the B and the sum of the momenta of the D_J and e candidates.) The hatching indicates the portion of each distribution that is selected by the cut.

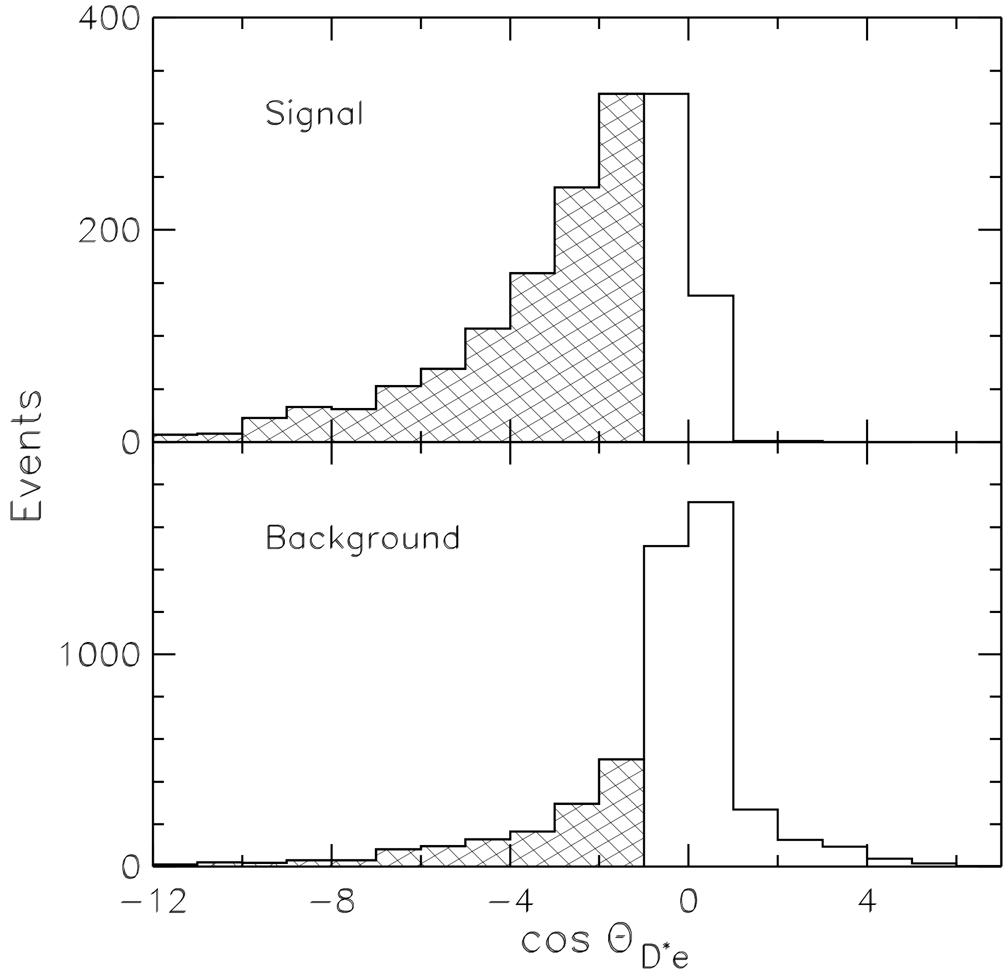

Figure 2: The value of $\cos\theta_{D^*e}$ is plotted for tagged signal events and generic Monte Carlo background from the $D^0 \to K^-\pi^+$ mode. (The angle θ_{D^*e} is the angle between the momentum of the B and the sum of the momenta of the D^* and e candidates.) The hatching indicates the portion of each distribution that is selected by the cut.

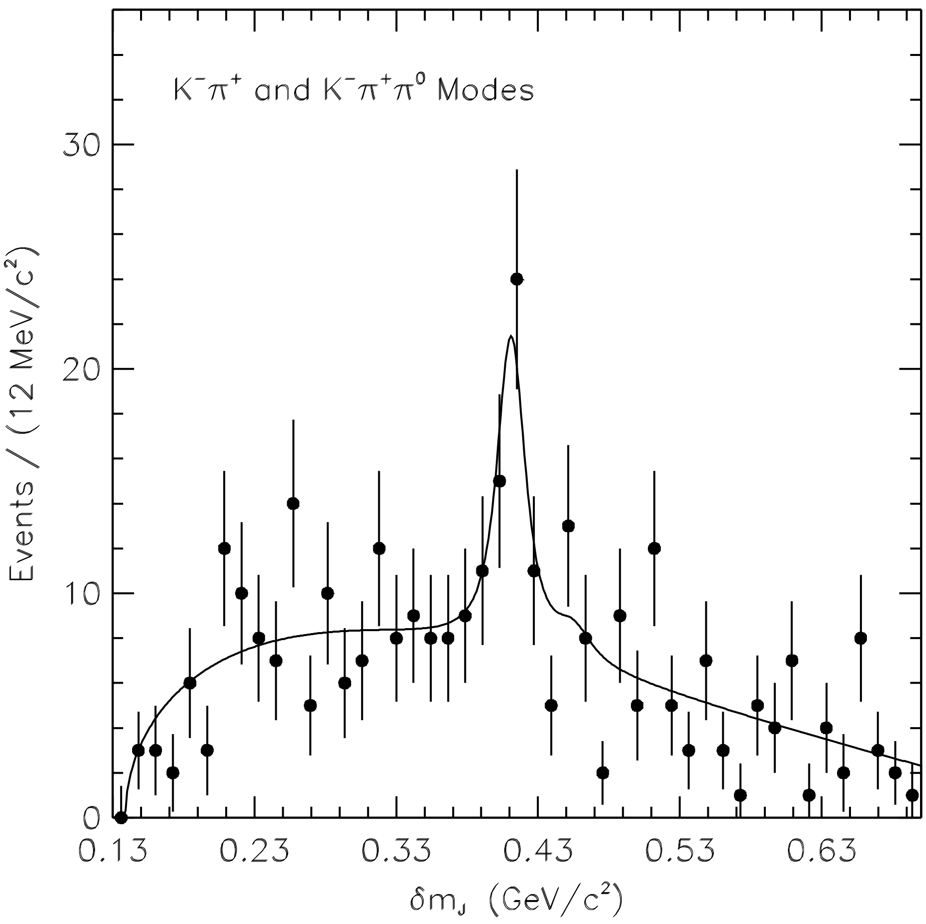

Figure 3: The δm_J distribution for $B^- \to D_J^0 e^- \bar{\nu}$ candidates, combining both the $D^0 \to K^-\pi^+$ and the $D^0 \to K^-\pi^+\pi^0$ modes.

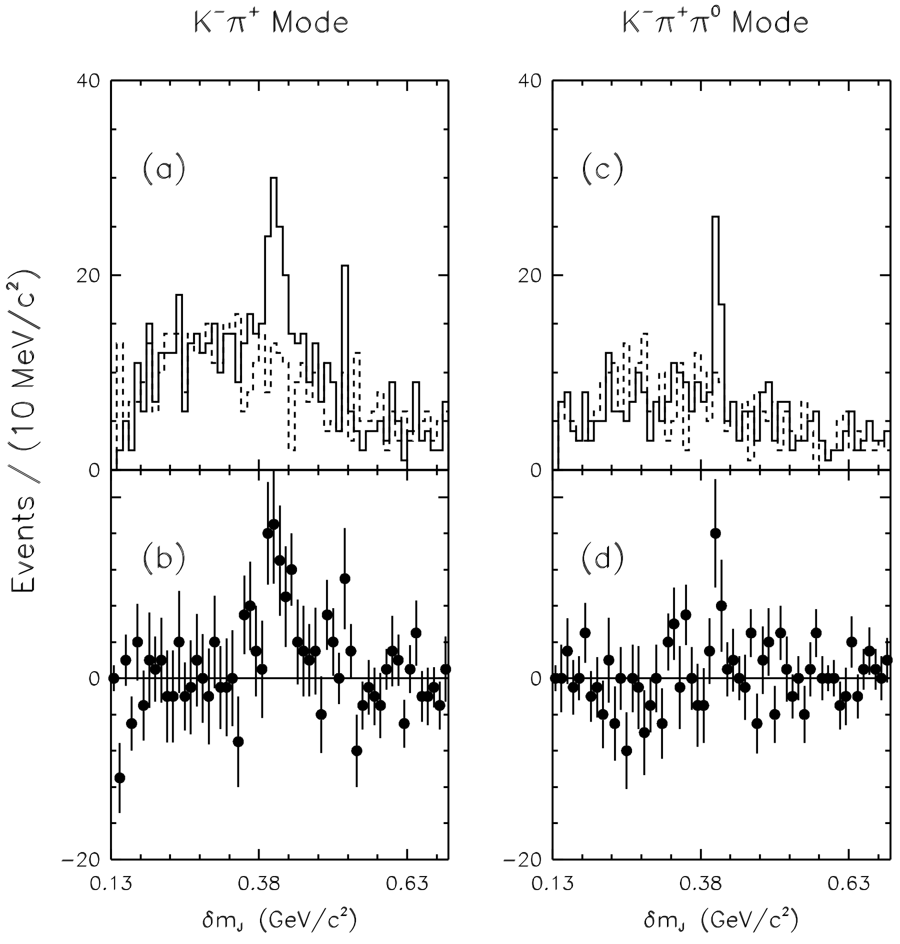

Figure 4: The δm_J distributions from generic Monte Carlo showing right sign ($D^{*+}\pi^-$) and wrong sign ($D^{*+}\pi^+$) combinations. Distributions (a) and (c) show the right sign as the solid line and the wrong sign as the dashed. Distributions (b) and (d) show wrong sign subtracted from right sign.

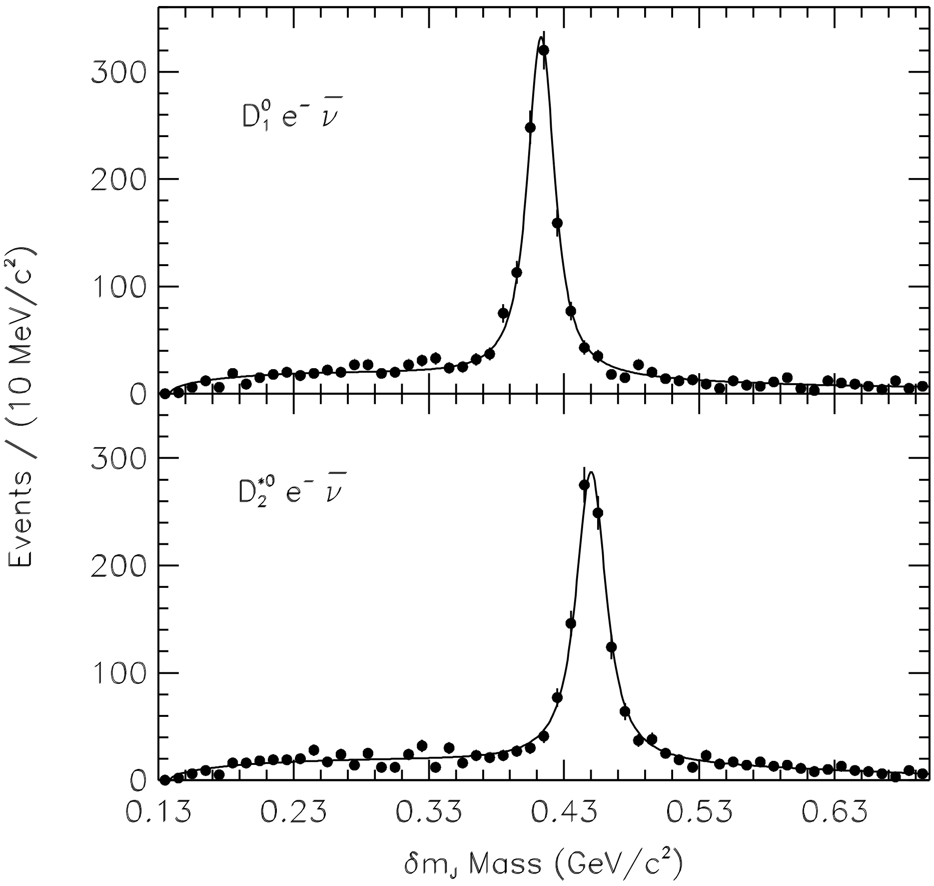

Figure 5: The δm_J distributions from signal Monte Carlo for $B^- \to D_1^0 e^- \bar{\nu}$ and $B^- \to D_2^{*0} e^- \bar{\nu}$ obtained by reconstructing the $D^0 \to K^- \pi^+$ mode. The distributions have been fit to a Breit-Wigner resonance convoluted with a Gaussian as described in the text. The yields were used to determine the efficiencies of our selection criteria.